Flash grab effect within the regions of modal and amodal completions

Hoko Nakada The University of Tokyo, Department of Psychology, Tokyo, Japan

Yuya Seshita The University of Tokyo, Department of Psychology, Tokyo, Japan

Haruka Shimazaki The University of Tokyo, Department of Psychology, Tokyo, Japan

Sohei Kito The University of Tokyo, Department of Psychology, Tokyo, Japan

Tomoya Nakamura The University of Tokyo, Department of Psychology, Tokyo, Japan; Center for Brain Science, Hirosawa, Wako-shi, Saitama, Japan; Japan Society for the Promotion of Science, Tokyo, Japan

Ikuya Murakami The University of Tokyo, Department of Psychology, Tokyo, Japan

When a rotating grating reverses its direction and is accompanied by a briefly flashed stimulus on top, the flash's apparent position shifts in direction after the reversal. This phenomenon, termed the *flash-grab effect*, can induce an illusory position shift of several degrees of visual angle, prompting investigation into scenarios in which the expected position coincides with another visual event. We investigated two such situations: perceptual filling-in at the blind spot and amodal completion behind a visible occluder. By inducing a position shift in the flash presented just outside such completed patterns, we measured the perceived angular position of the flash in the perceptual matching paradigm. We found subjective localization within the completed region of the moving inducer. Consistent results were found even when the flash was presented at a less optimal time for the flash-grab effect. Illusion size had a certain dependency on stimulus configuration, suggesting that various sources of spatial referencing are involved in the position processing around the blind-spot/occluder region. These findings imply that the visual system does not necessarily avoid a region that is devoid of physical motion stimuli when determining perceived flash position, reaching a consistent perceptual solution that integrates the motion-induced position shift and perceptual completion.

Introduction

Our visual environment typically has a coherent arrangement of objects evolving over time, maintaining causal relationships among neighboring elements. When a new object enters a scene, the visual system must seek evidence to establish its spatiotemporal relationship with existing objects, aiding in accurate identification and positioning. However, sudden visual events pose challenges because they may lack sufficient contextual cues for immediate localization within the surrounding space and time. Motion-induced position shifts serve as instructive examples of such perceptual challenges.

Various visual illusions underscore the intricate connection between motion and spatiotemporal position in perceptual organization, and the perceived position shifts in these phenomena have huge varieties

Citation: Nakada, H., Seshita, Y., Shimazaki, H., Kito, S., Nakamura, T., & Murakami, I. (2025). Flash grab effect within the regions of modal and amodal completions. *Journal of Vision*, *25*(3):4, 1–20, https://doi.org/10.1167/jov.25.3.4.

https://doi.org/10.1167/jov.25.3.4 Received August 19, 2024; published March 6, 2025 ISSN 1534-7362 Copyright 2025 The Authors

depending on motion contexts. In the Fröhlich effect, a stimulus appearing suddenly and initiating immediate motion at a constant speed causes its onset position to subjectively shift in the direction of motion (e.g., Müsseler & Aschersleben, 1998). Conversely, in onset repulsion, the onset position of a similarly moving stimulus appears to shift in the opposite direction (e.g., Thornton, 2002). Representational momentum presents another instance of positional mislocalization, wherein the offset position of a stimulus traveling a certain distance and suddenly disappearing shifts subjectively in the direction of motion (Freyd & Finke, 1984). Conversely, in offset repulsion, the offset position shifts subjectively in the opposite direction (Müsseler, Stork, & Kerzel, 2008). These opposing illusory position shifts between the Fröhlich effect and onset repulsion and between representational momentum and offset repulsion are contingent upon contextual factors (Müsseler & Kerzel, 2004; Merz, Soballa, Spence, & Frings, 2022).

The mutual connection between motion and position is also evident in positionally uncertain flashes that do not belong to motion patterns. That is, illusory position shifts manifest not only within moving stimuli themselves but also in independent visual stimuli briefly flashed amidst the presentation of other moving stimuli. The flash-drag effect (FDE) illustrates this phenomenon, wherein a flash suddenly presented near a drifting grating appears to shift in the direction of motion (Whitney & Cavanagh, 2000). The magnitude of this effect peaks when the flash and moving stimulus are separated by a few degrees of visual angle (dva) (Durant & Johnston, 2004), yet persists even at separation of up to 20 dva (Whitney & Cavanagh, 2000). Furthermore, the FDE occurs even when the flash and moving stimuli are presented dichoptically (Whitney & Cavanagh, 2000). Notably, subjective global motion from an array of random Gabor patches (Scarfe & Johnston, 2010) and implied motion occluded from view can also induce the FDE, albeit disappearing under conditions of suppressed motion awareness via binocular rivalry (Watanabe, 2005). Although these findings suggest involvement of higher-order processes with explicit representations of moving objects, the FDE can also arise from random motions in unpredictable directions (Fukiage, Whitney, & Murakami, 2011), suggesting that higher-order trajectory tracking is not imperative for the manifestation of this illusion.

Cavanagh and Anstis (2013) discovered another visual illusion, the flash-grab effect (FGE), capitalizing on a positional underestimation of up to 35% at the point of directional reversal of a moving stimulus (Sinico, Parovel, Casco, & Anstis, 2009). In the FGE, a circularly configured grating rotating at a constant angular velocity is accompanied by a flash atop it at the moment of the periodic reversal of its rotation direction. This causes the flash to appear to shift in the direction after the reversal by up to 10° of polar angle, as if "grabbed" by the grating. Experimental data suggest that attention plays a pivotal role in the occurrence of FGE (Cavanagh & Anstis, 2013; Adamian & Cavanagh, 2024), with predictability of directional reversals amplifying its magnitude (Coffey et al., 2019), implicating involvement of higher-order processes. Conversely, van Heusden, Harris, Garrido, and Hogendoorn (2019) reported that dichoptic presentation diminishes but does not abolish the FGE, suggesting involvement of mechanisms at both monocular and binocular stages. The distinctive characteristic of the FGE, compared to other phenomena involving motion-induced position shifts, lies in the robustness of its dramatic illusory shift, rendering it a promising tool for investigating the quantitative relationship between motion and position in intricate experimental scenarios.

As noted earlier, the visual system computes object positions, which can be heavily influenced by motion signals, yet faces constraints due to input signal layout and the biological architecture of the visual system itself. How does the visual system consistently interpret the position of a briefly flashed stimulus within these constraints? The FGE, characterized by its substantial magnitude and robustness, provides a valuable opportunity to explore this inquiry. Specifically, we seek to determine where a flash is subjectively localized if the "FGE prediction," the illusory position where the flash is expected to be localized because of the FGE, is already occupied by another "obstacle" potentially inconsistent with the solution of the position shift. Does the flash's perceived position avoid the obstacle? Are their positions integrated perceptually? Or does the flash exhibit a typical position shift regardless of the obstacle?

We introduce two types of obstacles. First, we confront the position shift with perceptual filling-in at the natural blind spot by inducing the FGE in the blind-spot direction. The blind spot is the region in the visual field corresponding to the optic disk in the eyeball, a structure occupied by blood vessels and ganglion cell axons that converge into the optic nerve. Lacking classical photoreceptors, the optic disk presents a gap in visual information. Despite this, observers remain unaware of the blind spot because processes for perceptual filling-in infer the content of the blind spot from surrounding information (Ramachandran, 1992). Maus and Whitney (2016) demonstrated that a grating vertically straddling the blind spot exhibited more accurate perception of spatial frequency in moving compared to static conditions, suggesting spatiotemporal filling-in of luminance modulation within the blind spot. When the FGE is induced by a rotating grating straddling the blind spot, is the flash subjectively localized within an illusory modulation completed within the blind spot? Alternatively, does such an unconventional perceptual solution of flash localization within the blind spot get rejected due to lack of sensory evidence? If so, where should the flash be subjectively localized within the visual field?

Second, we confront the position shift with a depth-order organization involving occlusion by overlaying the region around the FGE prediction with another static surface stimulus partially occluding the rotating grating. In the presence of such an occluder, the FGE may not manifest as strongly, given the static occluder's presence as a strong frame of reference regarding position. Alternatively, the percepts of the occluder and FGE may find a way to coexist. Since classical theories of Gestalt psychology (Koffka, 1935; Köhler, 1938; Wertheimer, 1912), various strategies have been proposed to resolve interrelationships among visual objects in response to specific sets of visual input signals. These include modal and amodal completions (e.g., Kanizsa, 1955; Kellman & Shipley, 1991), apparent transparency between objects (Metelli, 1985; Ware, 1980), and perceived depth order derived from occlusion depth cues such as T-junctions and accretion/deletion. If a mutually consistent perceptual solution based on these strategies aligns with the FGE prediction, could the FGE coexist with the recognition of amodal completion behind a visible occluder? Alternatively, might the FGE be confined within visible portions of the visual field, avoiding the occluder region as an obstacle?

This study delves into these inquiries through a series of experiments. On the screen, a circularly configured grating rotated at a constant angular velocity and reversed its rotation direction, with a red flash briefly presented atop it. The grating served as the inducer for the FGE, using three types of inducers: *filled-in*, *occluded*, and *physical*.

For the *filled-in* inducer, the inner and outer radii of the grating were configured so that the grating vertically straddled the blind spot of the right eye, never protruding horizontally beyond it. A blue ellipse consistently covered the blind-spot region, though invisible from the observer's viewpoint because of monocular observation with only the right eye open, resulting in a percept of a spatiotemporally filled-in grating via modal completion (Maus & Whitney, 2016). Inducing the FGE near the blind spot, we examined the subjective localization of the red flash.

For the *occluded* inducer, the same display was observed with both eyes open, making the blue ellipse visible as an occluder for the inducing grating. Utilizing the T-junctions and accretion/deletion as reliable depth cues, the inducer was perceived as partially covered by the ellipse but completed behind it via amodal completion. We induced the FGE near the occluder and assessed the subjective localization of the red flash. The occluder was constantly visible, potentially functioning as a frame of reference for the flash position. Under the above-described *filled-in* inducer condition, no such landmark was perceptually available. However, intrinsic information regarding the spatial extent of the blind spot might function as a reference frame for position (Ehinger, Häusser, Ossandon, & König, 2017). For the *physical* inducer, the spatiotemporal configuration remained identical, but the blue ellipse was omitted, allowing the rotating grating to be complete both physically and perceptually.

The red flash was presented either above or below the blind-spot region. The directional reversal of the inducer at the time of the flash onset was either clockwise (CW) to counterclockwise (CCW) or CCW to CW. Flash onset time was either synchronous or asynchronous with the directional reversal time. The FGE is maximized when the flash is presented synchronously with the directional reversal (Cavanagh & Anstis, 2013; Takao, Sarodo, Anstis, Watanabe, & Cavanagh, 2022); thus presenting the flash asynchronously during continuous motion may result in a smaller position shift. Although this smaller position shift in asynchronous timing can be understood as a weaker FGE, we also recognize the varied terminologies used for the phenomenon in the async condition—"asynchronous feature binding" (Cai & Schlag, 2001), "flash-jump illusion" (Sundberg, Fallah, & Reynolds, 2006), and "feature flash-drag effect" (Eagleman & Sejnowski, 2007). To assess the generalizability of our approach to the position perception shifted by the motion, we examined both optimal (synchronous) and suboptimal (asynchronous) conditions within the same experimental session. If intrusion into the blind-spot/occluder region is observed both in the synchronous and asynchronous conditions, the results would suggest that the two conditions simply produce stronger and weaker versions of a qualitatively identical illusion, namely the FGE. If the intrusion is observed only in one of the conditions, the results would be more compatible with the alternative view that the phenomenon in the async condition is qualitatively distinct from the classical FGE.

The research predictions are as follows. If the blind spot or physical occluder serve as static frames of reference disrupting the FGE, minimal or no position shift would be observed. Conversely, if they do not disrupt the FGE and perceptual consistency is maintained, the FGE would occur to the same extent as with the physical inducer. If the FGE is disrupted by the obstacles yet perceptual consistency is maintained, the FGE would occur to a lesser extent, possibly avoiding intrusion into the obstacle. Additionally, the FGE would be stronger with the filled-in than occluded inducer if the visibly completed presence of the inducer is crucial for its occurrence.

Methods

Participants

Nineteen adults (six males and thirteen females; aged 20–52 years) including one author with normal or corrected-to-normal vision participated. All participants except the author were naïve to the purpose of the experiment. Data from one individual were excluded due to unexpected equipment issues causing data collection failure. Two participants were unable to complete the practice sessions and therefore did not participate in the experimental sessions. Additionally, three participants withdrew before completing all repetitive experimental sessions, but their data were included in the following analysis because their exclusion did not alter the results and the collected data were unbiased in terms of sample distribution across tested conditions. Consequently, the following results and analyses were based on data from 16 participants. The study adhered to the Declaration of Helsinki guidelines. The experimental protocol received approval from the Ethics Committee of the Graduate School of Humanities and Sociology at the University of Tokyo and was conducted following approved guidelines. Each participant provided written informed consent before participation.

Apparatus

The experiment was conducted using a computer (Apple Mac Pro; Apple, Inc., Cupertino, CA, USA) running the MATLAB (MathWorks, Inc., Natick, MA, USA) programming environment, supplemented by the Psychophysics Toolbox (Brainard, 1997; Kleiner, Brainard, & Pelli, 2007; Pelli, 1997) and Eyelink Toolbox (Cornelissen, Peters, & Palmer, 2002) extensions. All the stimuli were presented on a 22-inch color CRT monitor (Mitsubishi Electric RDF223H; 1280 × 960 pixels; refresh rate 96 Hz; Mitsubishi Electric, Tokyo, Japan) in a dark room. A color-lookup table was used to correct for luminance linearity of the gamma profile. The viewing distance was fixed at 46 cm using a chin–forehead rest. For the filled-in inducer, participants viewed stimuli with only their right eye open, while the left eye was covered with an opaque eye patch. The gaze position of the right eye was recorded using an eye tracker (SR Research Eyelink CL; SR Research, Kanata, ON, Canada) at a sampling rate of 500 Hz.

Measurement of the position and size of the blind spot

The blind spot of each participant's right eye was identified at the beginning of the study to customize the stimuli in the subsequent practice and experimental sessions to fit the position and size parameters of each individual's blind spot.

Stimuli

On a black background, a central fixation point (a white-filled disk with a radius of 0.06 dva) and a red-filled ellipse were presented for the blind-spot measurement. To prevent Troxler fading, the ellipse was intermittently illuminated with an on-duty period of 625 ms and an off-duty period of 52 ms. Participants were able to manipulate the ellipse's position, akin to moving a mouse cursor, by using a computer mouse, while the major and minor diameters were adjusted using computer keys.

Procedure

With only the right eye open and the left eye occluded by an eye patch, each participant maintained fixation and adjusted the position and size of the ellipse to maximize the ellipse size while ensuring that it remained completely invisible.

Practice sessions for the perceptual matching of polar angle

Our goal was to quantify the FGE by perceptually matching the perceived position of the flash and that of a probe. Therefore, prior to the actual data collection, sufficient practice trials had to be conducted while monitoring the gaze position to confirm that the adjusted probe position accurately reflected the flash position when no illusion was present. To this end, a white annulus, red flash, and probe were presented in the practice trials without any moving stimuli that could influence the perceived position.

Stimuli

On a gray background (22.1 cd/m^2), a central fixation point (a bull's-eye composed of two black circles with radii of 1 dva and 0.5 dva) was always presented during each trial. A uniform white annulus (42.6 cd/m^2) was presented concentrically with the fixation point, occupying the same region as the custom-sized rotating grating in the subsequent FGE sessions (see below). Within the annulus, a red flat rectangle with a height of 1.5 dva and the same width as the annulus was flashed

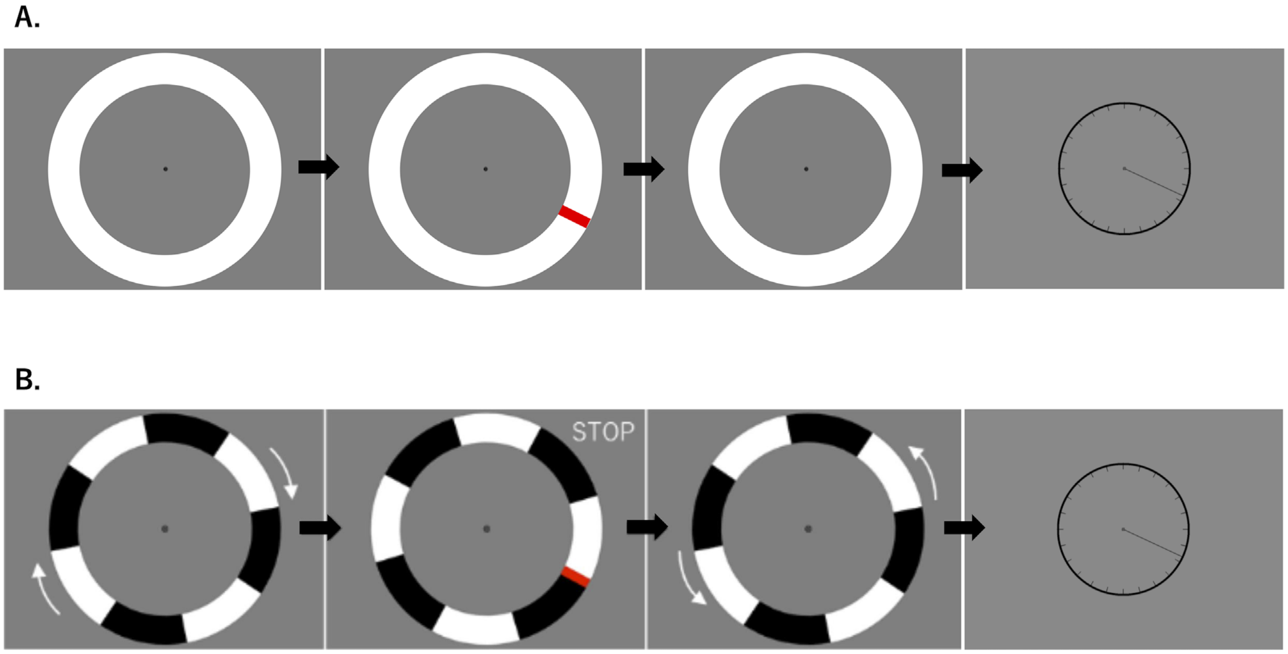

Figure 1. A stimulus sequence in a trial. (**A**) Practice session. A red flash was presented on a white annulus whose inner and outer radii were identical to those of the grating pattern in the FGE sessions. After the target and annulus disappeared, a black circle with tick marks was presented. (**B**) FGE session. A rotating grating was presented within an annular region. The grating initially rotated CCW or CW and subsequently rotated in the opposite direction. After the target and annulus disappeared, a black circle with tick marks was presented. The arrows and the word "STOP" are drawn for illustrative purposes here.

for 52 ms (Figure 1A). The polar angle of the flash was randomly chosen from −14°, −10°, −6°, −2°, 2°, 6°, 10°, and 14°, with zero indicating just rightward of the fixation point and the positive angles indicating CW direction. After the disappearance of the flash and annulus, a black circle (with a radius 60% of the annulus' inner radius) was presented concentrically with the fixation point. This circle was accompanied by black tick marks positioned at intervals of 15° along the polar angle, akin to a clock face with a tick mark every 0.5 hours. Additionally, a black rectangle was attached to the circle, akin to a clock hand, and its polar angle was freely adjustable, serving as the probe for perceptual matching.

Procedure

Each trial commenced with the onset of the fixation point accompanied by three beeps within approximately 0.6 second. One second after its onset, the annulus appeared, followed by the flash presented for 52 ms either 500 ms or 635 ms later. The annulus lasted for a total of 1052 ms. These temporal parameters were consistent with the FGE sessions (see below).

The disappearance of the annulus was followed by the onset of the clock. Participants were instructed to move the mouse to adjust the polar angle of the probe until it matched the flash's angle. Upon completing the adjustment and clicking the mouse, the point of subjective equality (PSE) in terms of polar angle was recorded, and a 500-ms visual feedback period ensued. During this period, the annulus and flash reappeared, accompanied by numerical feedback in degrees indicating the degree of clockwise deviation of the adjusted probe from the true polar angle of the flash.

In the first (familiarization) block, 32 trials (8 angles × 4 repetitions) were conducted. In the second (training) block, participants repeated trials until achieving six consecutive successful trials, defined as an angular deviation within ±3°. In the third (eye-tracking) block, the same procedure as the second block was repeated while the eye tracker monitored the right eye's gaze. If the gaze deviated beyond ±1 dva (or ±2 dva for some participants with suboptimal eye-tracking calibration) from the onset of the beep to the disappearance of the annulus, the trial was deemed unsuccessful and retried within the same session.

Experimental sessions for the perceptual matching of the flash-grab effect

Stimuli

On a gray background (27.6 cd/m^2), the same fixation point as in the practice sessions was presented in each trial. As the inducer, a rotating grating was

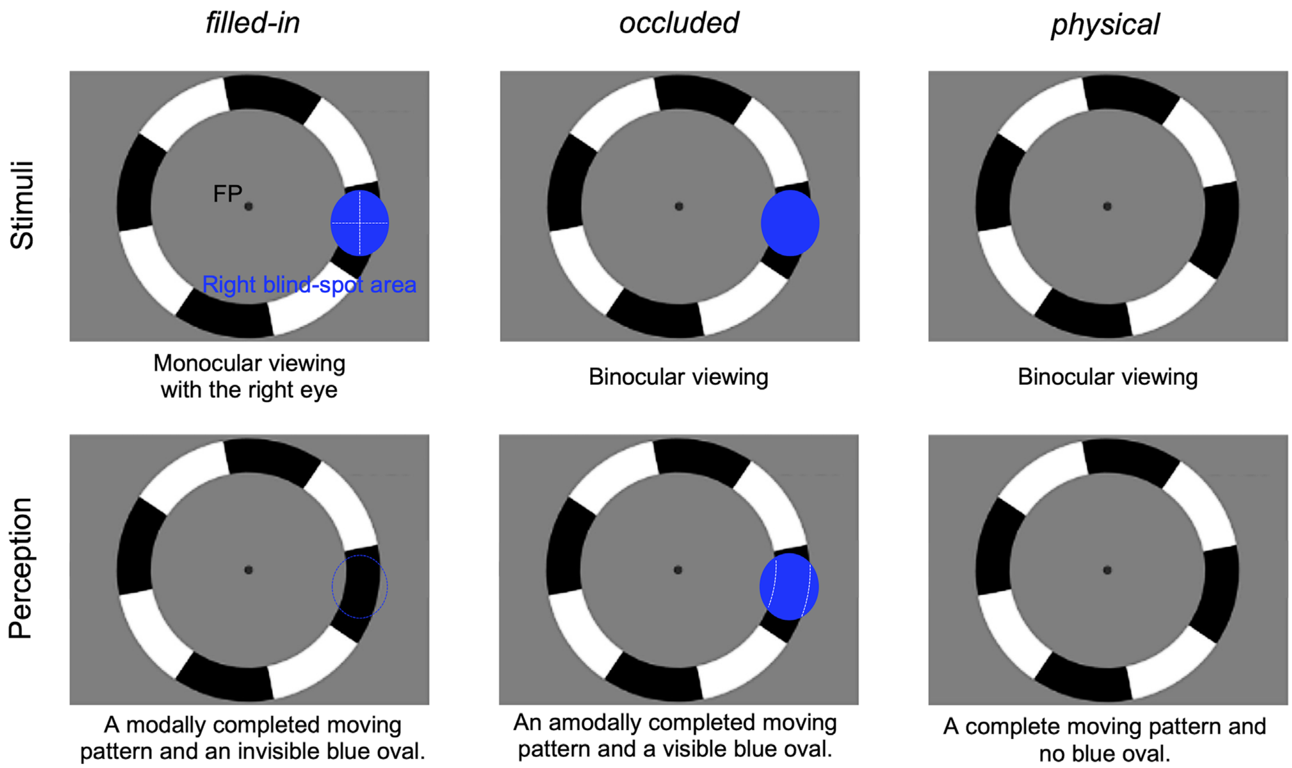

Figure 2. Three types of inducers (filled-in, occluded, and physical). The upper column shows stimulus configuration and the lower column shows perception. FP: fixation point.

presented within an annular region concentric with the fixation point (Figure 1B). The inducer comprised a square-wave luminance modulation (contrast 90%) as a function of polar angle at 4 cycles/circle. The radius of the annulus was near-equated to the eccentricity of the blind-spot center (Figure 2). The width of the inducer matched the width of the blind spot minus 2 dva, ensuring that the inducer passed through the inside of the blind spot without protruding horizontally. In each trial, the inducer rotated by 135° of polar angle at a constant speed of 270°/s for 500 ms, remained stationary for 52 ms, rotated in the reverse direction by 135°, again remained stationary for 52 ms, and then disappeared. In the CW condition, the inducer initially rotated CCW and subsequently rotated CW. In the CCW condition, the inducer initially rotated CW and subsequently rotated CCW (Figure 3A).

Superimposed on the inducer, a red flat rectangle with a height of 1.5 dva and the same width as the inducer was briefly flashed for 52 ms. The flash position was chosen from the *top* or *bottom* conditions in a random order. In the top condition, the flash was positioned −5° of polar angle above the top of the blind spot. In the bottom condition, the flash was positioned 5° below the bottom of the blind spot (Figure 3B). We placed the flash 5° away from the blind-spot border to ensure that the entire flash shape remained outside the blind spot at the input level and that the FGE prediction fell within the blind spot, as previously reported degrees of the FGE typically exceeded 5° (Cavanagh & Anstis, 2013).

The flash onset time was chosen from two candidates in a random order (see the Procedure section below); in the sync condition, the flash was superimposed on one of the inducer's luminance boundaries while the inducer remained stationary for 52 ms. In the async condition, the flash was superimposed on one of the luminance boundaries while the inducer continued rotating at a constant speed (Figure 3C). Because the flash remained stationary for 52 ms, it appeared 31 ms before the luminance boundary passed through the flash location, maintaining its position while the boundary passed during constant rotation.

In the case of the filled-in inducer (Supplementary Movie S1), a blue ellipse covering the blind spot covered the inducer but was invisible because, with only the right eye open, the region was perceptually filled-in with the inducer and background. For the occluded inducer (Supplementary Movie S1), the same blue ellipse was presented in the same manner but was visible because both eyes were open. For the physical inducer (Supplementary Movie S2), no such ellipse covering the inducer was presented and both eyes were open. For the perceptual matching task, the same clock with a hand, as used in the practice session, was used as the probe.

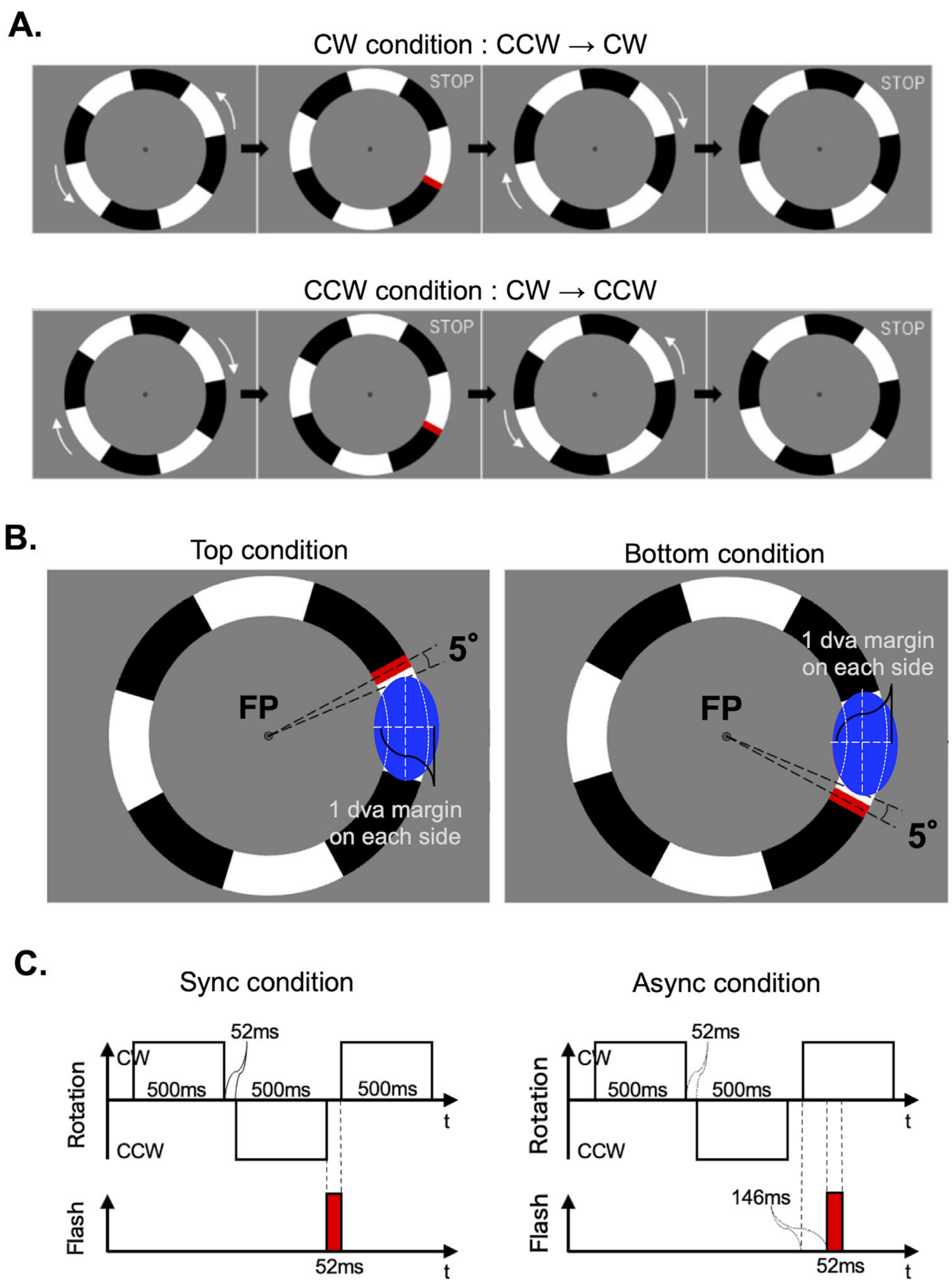

Figure 3. Stimulus conditions. For each inducer (see Figure 2), there were eight combinations of two rotation directions after the reversal (CW and CCW), two flash positions (top and bottom), and two flash onset times (sync and async). (**A**) Rotation direction. In the CW condition, the inducer initially rotated CCW and subsequently rotated CW. In the CCW condition, the inducer initially rotated CW and subsequently rotated CCW. (**B**) Flash position. In the *top* and *bottom* conditions, the flash position was −5° above the top, and 5° below the bottom, respectively, of the blind spot. (**C**) Flash onset time. In the sync condition, the flash was superimposed on one of the luminance boundaries while the inducer stayed stationary for 52 ms. In the async condition, the flash was superimposed on one of the luminance boundaries, while the inducer continued rotating at a constant speed.

Procedure

Each trial commenced with the onset of the fixation point accompanied by three beeps within approximately 0.6 second. One second after its onset, the inducer appeared, followed by the flash presented for 52 ms either 500 ms or 635 ms later. The inducer lasted for 1052 ms.

The disappearance of the inducer was followed by the onset of the clock. Participants were asked to adjust the polar angle of the probe, as in the practice sessions, but no feedback was provided.

The sessions for the *filled-in*, *occluded*, and *physical* inducers were conducted in separate blocks. For the *filled-in* inducer, each block commenced with the presentation of a grating and flickering blue ellipse to confirm that the grating was perceptually completed while the ellipse remained invisible. Each block consisted of 56 trials (2 flash positions [top and bottom] × 2 flash onset times [sync and async] × 2 rotation directions after reversal [*CW* and *CCW*] × 7 repetitions). Throughout all trials, the eye tracker monitored the right eye's gaze. If the gaze deviated beyond ±1 dva (or ±2 dva for some participants with suboptimal eye-tracking calibration) from the onset of the beep to the disappearance of the annulus, the trial was deemed unsuccessful and retried within the same block. Regardless of fixation success or failure, a brief break was inserted after every 30 consecutive trials. Four such blocks were intermingled for the three inducer types, with the order counterbalanced across participants. Therefore the PSE for each condition was based on the data from 28 repetitive trials.

Results

Individual data

For the perceived position of the flash, presented either synchronously (sync) or asynchronously (async) with the directional reversal of the inducer, the PSE is depicted in Figure 4 for a representative participant, whereas results for other individuals are detailed in the Supplementary Information (Supplementary Figures S1 and S2). In each panel, the gray bar indicates the physical position of the flash, while the blue, cyan, brown, and orange bars indicate the average PSE data in the top-CCW, top-CW, bottom-CCW, and bottom-CW conditions, respectively. For each condition, a one-sample two-tailed t-test confirmed that the position shift, consistent with the occurrence of FGE, was >0° (Supplementary Tables S1 and S2). In the top-CW and bottom-CCW conditions, in which the FGE prediction fell within the ellipse blind-spot region, another one-sample two-tailed t-test was performed to determine if the PSE was >5° in polar angle. Given that the flash was presented 5° away from the border of the ellipse, a PSE >5° implied the occurrence of FGE extending beyond the distance between the physical flash position and the ellipse border and into the interior of the ellipse. The results indicated that, for these two participants, the perceived position was indeed localized within the blind-spot region with the *filled-in* and *occluded* (Supplementary Tables S3 and S4) inducers, at least in the bottom-CCW condition.

Group data

Figure 5 shows within-observer averages (circles) and inter-observer averages (bars) for all 16 participants. The ordinate represents angular mislocalization, where the positive shifts denote the CCW direction.

For the interobserver averages, we performed one-sample t-tests to determine whether the FGE shift (i.e., the angular mislocalization in the direction of the FGE prediction) was >0° to confirm the occurrence of FGE. In the sync condition with the filled-in inducer, the FGE shift was >0° in the top-CCW ($t(15) = 2.16$, $p = 0.047$), top-CW ($t(15) = 6.17$, $p < 0.001$) and bottom-CCW ($t(15) = 11.45$, $p < 0.001$) conditions, although the shift in the top-CCW condition was not significant after the adjustment of significance level using the Holm method. In the sync condition with the occluded inducer, the FGE shift was >0° in the top-CCW ($t(15) = 2.86$, $p = 0.012$), top-CW ($t(15) = 6.00$, $p < 0.001$), and bottom-CCW ($t(15) = 7.68$, $p < 0.001$) conditions. In the async condition with the filled-in inducer, the FGE shift was >0° in the top-CW ($t(15) = 6.45$, $p < 0.001$) and bottom-CCW ($t(15) = 7.80$, $p < 0.001$) conditions. In the async condition with the occluded inducer, the FGE shift was >0° in the top-CW ($t(15) = 6.08$, $p < 0.001$) and bottom-CCW ($t(15) = 7.94$, $p < 0.001$) conditions. Thus, in all combinations of inducer type (filled-in and occluded) and flash onset time (sync and async), the FGE significantly occurred at least in the critical conditions in which the FGE prediction was within the blind-spot region. In all conditions with the physical inducer, the FGE shift was >0° (the async and top-CCW, $p = 0.011$; the async and bottom-CCW, $p = 0.038$; otherwise, ps < 0.001).

As mentioned in the above individual data analysis, the FGE prediction under the bottom-CCW and top-CW conditions fell inside the blind-spot region. To examine whether the FGE indeed delivered the flash inside the blind-spot region in the critical conditions of bottom-CCW and top-CW, we performed a one-sample two-tailed t-test to determine whether the FGE shift was >5°, i.e., the distance between the flash and the ellipse border, for the inter-observer average in each condition. The results were as follows.

(1) In the sync condition with the filled-in inducer, the FGE shift was >5° in the bottom-CCW condition ($t(15) = 5.74$, Holm-corrected $p < 0.001$, $r = 0.83$), but not in the top-CW condition (n.s.).
(2) In the sync condition with the occluded inducer, the FGE shift was >5° in the bottom-CCW condition ($t(15) = 3.32$, Holm-corrected $p = 0.009$, $r = 0.65$), but not in the top-CW condition (n.s.).
(3) In the sync condition with the physical inducer, the FGE shift was >5° in the bottom-CCW

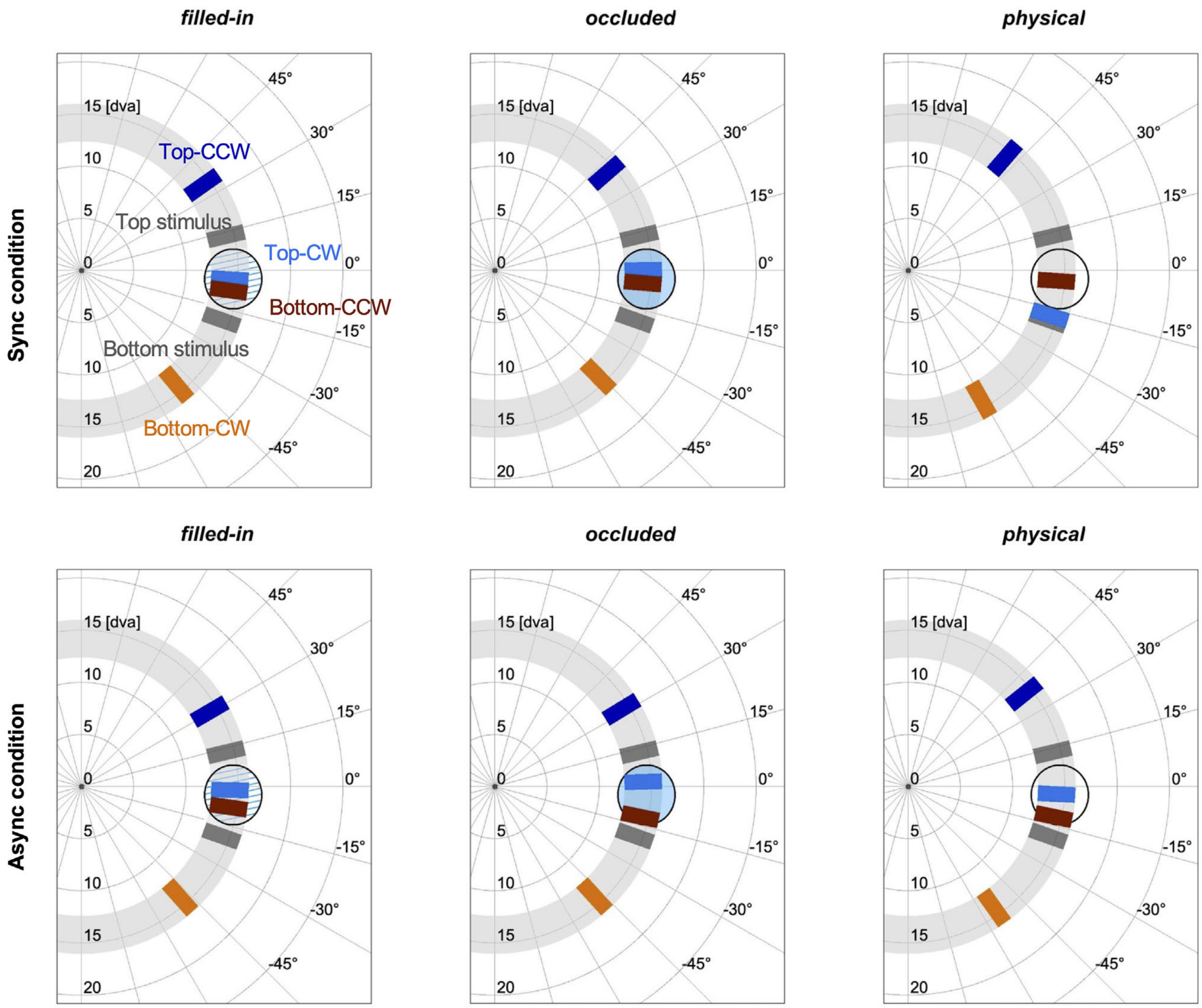

Figure 4. Examples of individual data. (Upper row) PSEs for a naïve observer in the sync condition. In polar coordinates, the pole represents the fixation point (FP), and the radial distance represents the eccentricity in degrees of visual angle (dva) from the FP. Polar angles (°) are defined relative to the horizontal meridian. In each panel, the gray annulus and two gray bars indicate the inducer track and the physical flash positions (top and bottom), respectively. The blue, cyan, brown, and orange bars indicate the average PSE data in the top-CCW, top-CW, bottom-CCW, and bottom-CW conditions, respectively. The open black ellipse indicates the right eye's blind spot identified individually prior to the experimental sessions. For the filled-in inducer (in monocular viewing with the right eye), this region (striped blue fill) was occupied by a blue ellipse but it was rendered invisible by filling-in. For the occluded inducer (in binocular viewing), the blue ellipse occupying this region (blue fill) was visibly occluding the inducer. For the physical inducer, no ellipse was presented on the screen, and an elliptic frame is depicted here for only illustrative purposes as a comparison with other conditions. In all the conditions, the PSE was significantly different from 5° in the polar angle. (Lower row) PSEs for the same naïve observer in the async condition. The conventions are identical to those of panel A. In all the conditions, the PSE was significantly different from 5° in the polar angle.

condition ($t(15) = 6.45$, Holm-corrected $p < 0.001$, $r = 0.86$) and the top-CW condition ($t(15) = 4.07$, Holm-corrected $p = 0.001$, $r = 0.72$).

(4) In the async condition with the filled-in inducer, the FGE shift was $>5°$ in the bottom-CCW condition ($t(15) = 3.34$, Holm-corrected $p = 0.01$, $r = 0.66$), but not in the top-CW condition (n.s.).

(5) In the async condition with the occluded inducer, the FGE shift was $>5°$ in the bottom-CCW condition ($t(15) = 2.77$, Holm-corrected $p = 0.03$, $r = 0.58$), but not in the *top-CW* condition (n.s.).

(6) In the async condition with the physical inducer, the FGE shift was $>5°$ in neither the bottom-CCW condition (n.s.) nor the top-CW condition (n.s.).

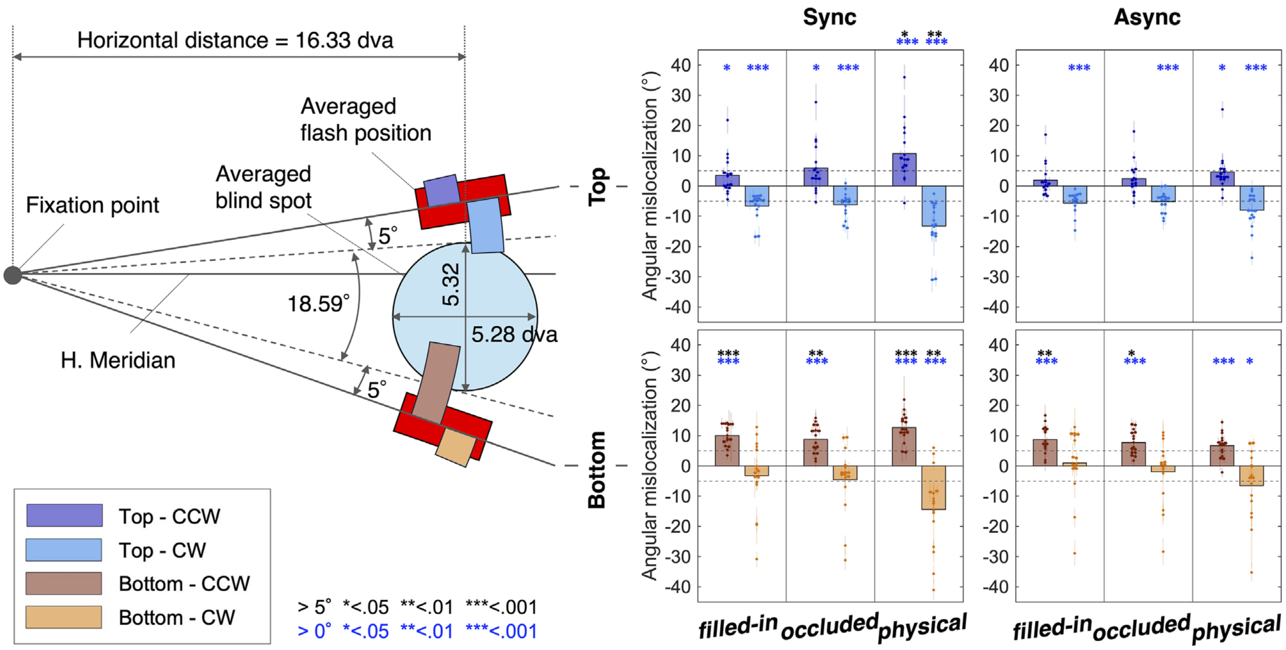

Figure 5. Group data. (Left) Average blind-spot size and horizontal distance from the fovea for the 16 observers. The bar charts depict angular mislocalization data in the sync condition with the filled-in inducer (i.e., the charts shown in the first column of the right panel). (Right) Average mislocalization for the 16 observers. The circles and thin lines indicate each observer's average angular mislocalization and the 95% confidence interval. For the top-CW and bottom-CCW conditions, in which the FGE prediction was inside the blind-spot region, it was meaningful to compare the data with 5°, and this level is indicated by the broken line. The blue and black asterisks indicate the conditions in which the FGE shift was significantly different from 0° and 5°, respectively (*$P < 0.05$; **$P < 0.01$; ***$P < 0.001$).

To compare the FGE shifts across conditions, we additionally performed a four-way repeated-measures analysis of variance (ANOVA) with inducer type (filled-in, occluded, and physical), flash onset time (sync and async), flash position (top and bottom), and rotation direction after the reversal (CW and CCW) as factors. The main effect of flash onset time ($F(1,15) = 47.44$, $p < 0.001$, $\eta_p^2 = 0.76$) was significant, confirming that the FGE shift indeed depended on the synchronicity between the flash and the directional reversal of the inducer, consistent with previous studies (Cavanagh & Anstis, 2013). The main effect of inducer type ($F(2,30) = 26.89$, $p < 0.001$, $\eta_p^2 = 0.64$) was significant. Because there was no significant four-way interaction ($p = 0.75$), we further analyzed the sync and async conditions separately using a three-way ANOVA for each, with completion type, target position, and rotation direction as the factors. In the sync condition, in which an optimal FGE was expected to occur, the main effect of completion type was significant ($F(2,30) = 32.07$, $p < 0.001$, $\eta_p^2 = 0.68$). The statistical results for other conditions including the async condition are detailed in Tables 1 and 2. In the results of the post-hoc pairwise multiple comparisons with the Tukey-Kramer method, the illusion amplitude for the filled-in inducer was significantly smaller than that for the physical inducer in the *top-CCW* condition ($t(15) = 5.03$, $p < 0.001$, $r = 0.79$). In the top-CW condition, the filled-in ($t(15) = 4.65$, $p < 0.001$, $r = 0.77$) and occluded ($t(15) = 4.94$, $p < 0.001$, $r = 0.79$) inducers exhibited significantly smaller illusion amplitudes than the physical inducer.

Distribution of illusory position shifts

To further elucidate the distribution of illusory position shifts, we examined whether the average FGE shift accurately represented the perceived flash position inside the blind-spot region. There was a possibility that the average shift did not accurately reflect the distribution if the perceived position obeyed a bimodal distribution, with some data points clustering near the bottom border of the blind spot and others near the top border. To investigate this, we plotted the PSE for each trial on a size-normalized blind-spot region on an individual basis (Figure 6). In the sync and async conditions for the filled-in and occluded inducers, the PSE fell well within the blind-spot region for at least nine to 13 out of 16 participants. For the other participants, the PSE was more widely distributed,

Sync condition	*df*	*F*	*p*	η_p^2
Completion type	2,30	32.066	<0.001	0.681
Target position	1,15	4.009	0.064	0.211
Rotation direction	1,15	0.274	0.608	0.018
Completion type * Target position	2,30	0.56	0.577	0.036
Completion type * Rotation direction	2,30	6.716	0.004	0.309
Target position * Rotation direction	1,15	1.682	0.214	0.101
Completion type * Target position * Rotation direction	2,30	6.115	0.006	0.29

Table 1. Results of the ANOVA for the main effects, two-way interactions, and three-way interactions (sync condition). The asterisk denotes an interaction effect between factors.

Async condition	*df*	*F*	*p*	η_p^2
Completion type	2,30	14.979	<.001	0.5
Target position	1,15	0.944	0.347	0.059
Rotation direction	1,15	0.533	0.477	0.034
Completion type * Target position	2,30	0.903	0.416	0.057
Completion type * Rotation direction	2,30	12.052	<.001	0.446
Target position * Rotation direction	1,15	4.596	0.049	0.235
Completion type * Target position * Rotation direction	2,30	9.514	<.001	0.388

Table 2. Results of the ANOVA for the main effects, two-way interactions, and three-way interactions (async condition). The asterisk denotes an interaction effect between factors.

but there was no indication of bimodality. Thus these results confirm that the FGE was able to deliver the perceived flash position into the blind-spot region.

Uncompleted inducer

Before drawing a conclusive remark, another logical possibility must be considered; whether perceptual completion was necessary for the observed pattern of results, or if the physical visual input of the inducer alone was sufficient to produce the illusory position shift. To address this possibility, we conducted a subsidiary experiment wherein the inducer was modified to eliminate any possibility of completion. The upper right part of the original inducer was reshaped as a straight horizontal line, termed the uncompleted inducer (Supplementary Movie S3). The length of this straight part matched the length of the arc that would occupy the upper right part of the original inducer. Unlike in the main experiment, the blind-spot region was left blank, and the stimulus was viewed with both eyes open. Consequently, there was no perceptual completion of the inducer. Additionally, we replicated the physical inducer from the main experiment to verify whether the FGE occurred in a more typical configuration.

Each block consisted of 56 trials (2 flash onset times [sync and async] × 2 rotation directions after the reversal [CW and CCW] × 14 repetitions). The flash presentation location was fixed at the bottom, resulting in only the bottom-CW and bottom-CCW conditions being considered. The uncompleted and physical inducers were used in separate blocks. Regardless of fixation success or failure, a brief break was inserted after every 30 consecutive trials. Two such blocks were intermingled for the two inducer types, with the order counterbalanced across participants. The PSE for each condition was based on the data from 28 repetitive trials.

In the sync condition, all three participants (aged 25–30 years with normal or corrected-to-normal vision) yielded the same results (Figure 7). In the bottom-CCW condition with the physical inducer, all participants showed a shift >5° (P3, the mean of FGE (M_{FGE}) was 12.01°, $t(27) = 8.41$, $p < 0.001$; P17, $M_{FGE} = 18.55$, $t(27) = 13.70$, $p < 0.001$; P18, $M_{FGE} = 14.41$, $t(27) = 10.64$, $p < 0.001$). However, with the uncompleted inducer, the shifts did not exceed 5° significantly in any conditions (P3, $M_{FGE} = 3.68$, $t(27) = -2.54$, $p = 0.02$; P17, $M_{FGE} = 4.87$, $t(27) = -0.28$, $p = 0.78$; P18, $M_{FGE} = 1.20$, $t(27) = -6.55$, $p < 0.001$). Similar results were obtained in the async condition (Supplementary Tables S5 and S6).

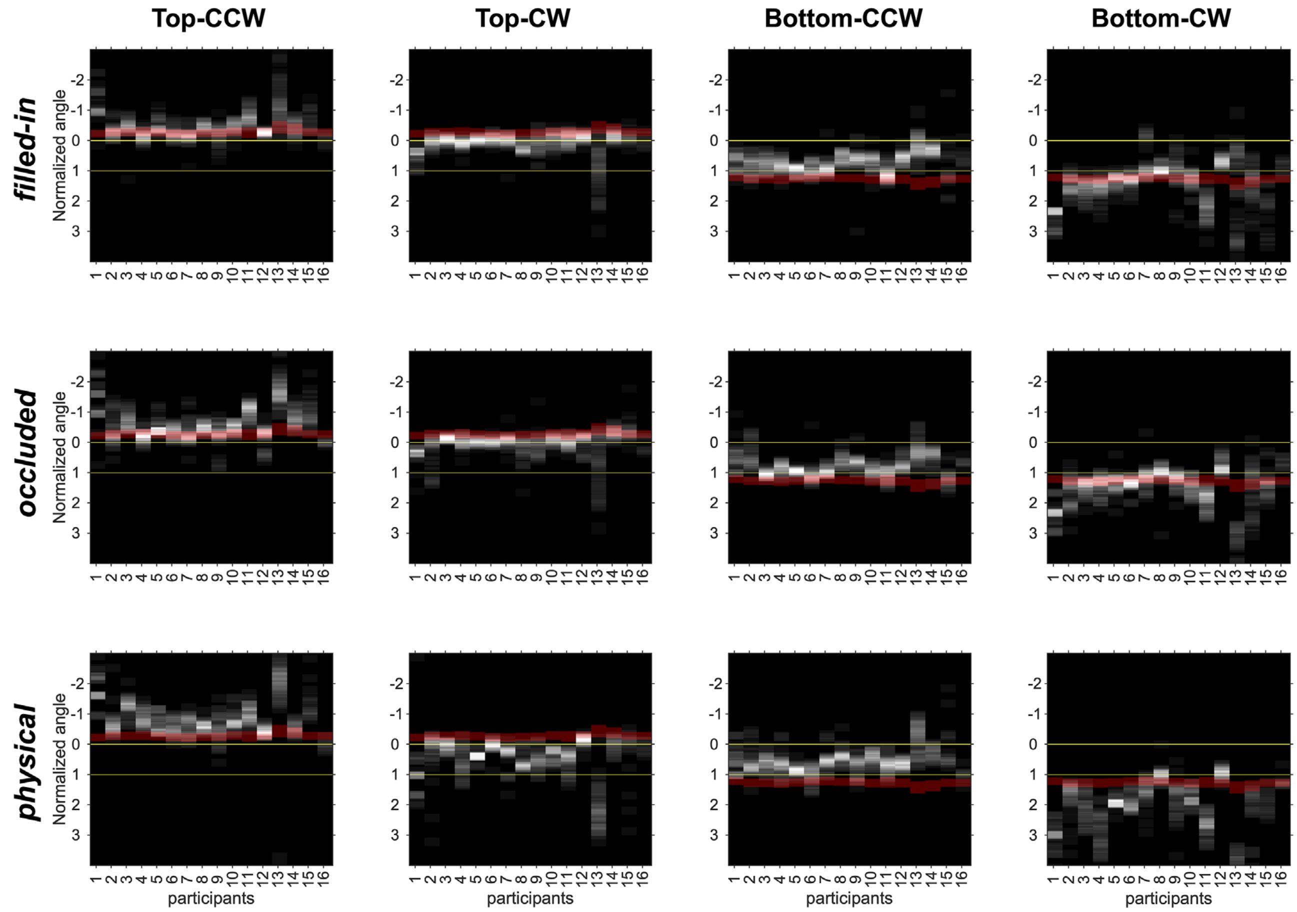

Figure 6. Trial-by-trial data in the sync condition for the 16 participants, plotted at a normalized height of the blind spot for each participant. 0 and 1 mean the polar angle of the top and bottom of the blind-spot region, respectively (yellow lines). The ordinate indicates the PSE in polar angle, not FGE shift, unlike in Figure 5, and thus the downward and upward directions correspond to the CW and CCW directions on the screen, respectively. The red bars indicate the true flash position and the white bars indicate the PSE in each trial. The brighter positions indicate that the responses were concentrated more densely.

Discussion

Summary of the results

This study yielded five main findings:

(1) When the inducer was modally completed (filled-in) within the blind spot, the FGE from the bottom to the inside of the blind spot (bottom-CCW) was observed whereas the FGE from the top to the inside (top-CW) was not.
(2) When the inducer was amodally completed (occluded) behind an occluder, the FGE from the bottom to the inside (bottom-CCW) was observed whereas the FGE from the top to the inside (top-CW) was not.
(3) The FGE into the completed region was smaller than that obtained in a more classical (physical) condition when the flash timing was optimal (sync) for FGE occurrence.
(4) There was no significant difference in the illusion size between the modally and amodally completed regions.
(5) Unless noted otherwise, these relationships were consistently observed whether the flash was synchronous (sync) or asynchronous (async) with the directional reversal although, as in previous studies, FGE was larger when the flash was presented synchronously compared to when presented asynchronously.

These characteristics summarized the inter-observer average for the 16 participants (Figure 5) and are also seen in the within-observer data for many of the participants (Supplementary Figures S1 and S2). FGE from the bottom to the inside of the blind spot (filled-in, bottom-CCW) was observed in at least 12 of the 16 participants. FGE from the bottom to the inside of the

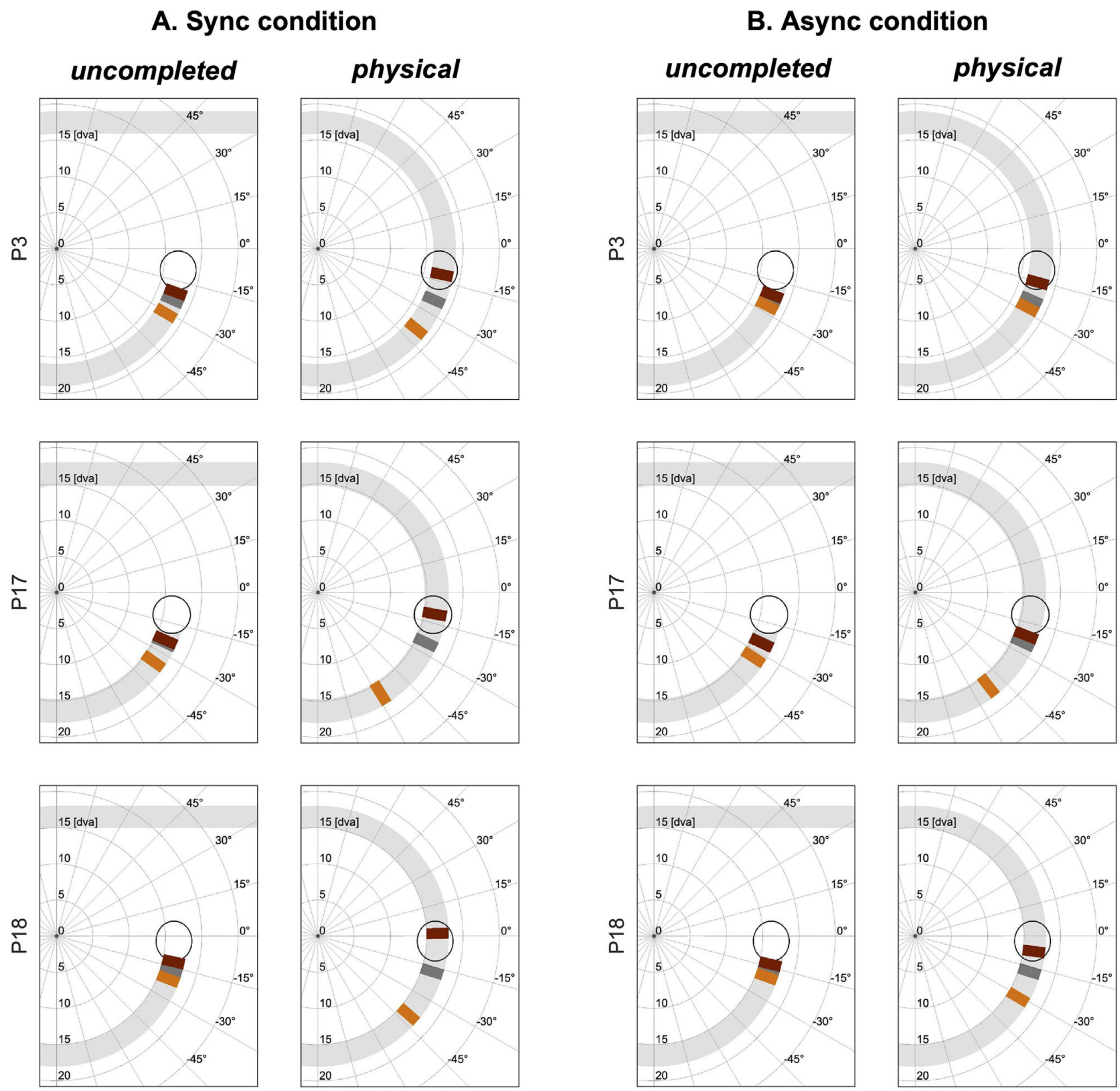

Figure 7. PSEs for three naïve observers in the subsidiary experiment. The conventions are identical to those of Figure 4.

occluder (occluded, bottom-CCW) was observed in at least 12 of the 16 participants (Supplementary Tables S3 and S4). These findings demonstrate that, at least in the majority of conditions in which the FGE prediction was inside the blind-spot region, neither the blind spot nor the occluder worked as an "obstacle" that would prohibit the occurrence of FGE inside, although they might play a role in the reduction of FGE.

In the sync condition, the inducer's locally moving edge just outside the ellipse traversed for the rotation angle of 5° after the flash presentation and before moving into the ellipse region, and this counts to only two display frames long (20.83 ms). Thus the local edge is assumed to be perceptually completed within the blind-spot area to provide the rest of the amount of illusion (approximately 5° for the filled-in and occluded inducers). Furthermore, the information on global rotation, which provides a rich spatiotemporal context for this phenomenon to occur optimally (Cavanagh & Anstis, 2013), is considered an important factor besides the information on the locally moving edge. The occurrence of the FGE requires both the global motion and local spatial alignment of the inducer because the FGE amplitude decreases as the flash position deviates from the inducer's luminance edge (Cavanagh & Anstis, 2013). As such, the smaller FGE amplitudes in the filled-in and occluded conditions than in the physical condition (Figure 5) may be partly explained by the temporally limited availability of the visual input of the local luminance edge at the flash position, with rich global motion information left intact.

Hierarchy of processes

The flash position shifting inside the blind spot suggests that the process for modal completion precedes the process for the FGE because within a processing stage where the inducer representation is missing due to the retinal defect, there is no candidate carrier to "grab" the flash into the missing part and localize it therein. Maus and Nijhawan (2008) demonstrated that a stimulus moving toward the blind spot can be localized within it. Their observers were asked to judge the final position of a bar moving into the blind spot, and the bar was perceived to disappear in positions well inside the blind spot when sensory evidence for the position of disappearance was unavailable. Taken together, it is plausible that even in monocular viewing, the visual system is capable of object localization within the blind spot. Furthermore, the absence of FGE invasion into the blind spot when no completion occurred (i.e., uncompleted) indicates the necessity of perceptual completion for the FGE to occur within the blind spot, contrasting with the perceived final position of the moving bar in Maus and Nijhawan's study, in which perceptual completion was indeed established.

Past studies aiming to identify the neural correlates of perceptual completion at the blind spot suggest the involvement of a hierarchy of processing stages including area V1 and beyond. Although the region corresponding to the blind spot in area V1 contains neurons with characteristics functionally suitable for surface filling-in, such as large binocular receptive fields extending beyond the blind spot (Komatsu, Kinoshita, & Murakami, 2000; Komatsu, Kinoshita, & Murakami, 2002), neural activity evoked by the stimulation of one side of the blind spot does not automatically "infiltrate" within the blind-spot region, inconsistent with passive remapping theory (Awater, Kerlin, Evans, & Tong, 2005; Matsumoto & Komatsu, 2005). Functional magnetic resonance imaging studies for area V1 have demonstrated ipsilateral ocular dominance within the blind-spot region (de Hollander, van der Zwaag, Qian, Zhang, & Knapen, 2021) and accurate reconstruction of the spatial extent of an participant's blind spot using the population receptive field protocol (Urale, Puckett, York, Arnold, & Schwarzkopf, 2022). In monkey neurophysiology, the time course of neural responses to stimuli inducing perceptual completion at the blind spot suggests that the formation of cortical representations pertinent to completion requires communications across the hierarchy of neural processing between V1 and higher areas, rather than horizontal propagation within V1 (Matsumoto & Komatsu, 2005). Thus it is plausible that computations supporting perceptual filling-in at the blind spot have not yet been completed in area V1, as evidenced by the retinotopic map of the blind spot in the form of a large continuous cortical region of ocular dominance for the fellow eye (Komatsu et al., 2000; Komatsu et al., 2002) but have been established in early visual areas containing retinotopic organizations that are sufficiently precise to localize the flash position that was psychophysically quantifiable with the method of perceptual matching in terms of polar angle, as in the present study.

The findings of the present study are also consistent with the view that the underlying mechanism of the FGE involves higher-order processes compatible with active inference on the spatiotemporal localization of an abrupt stimulus based on attentional monitoring (Cavanagh & Anstis, 2013; Adamian & Cavanagh, 2024). Beyond areas V1 and V2, the dorsal stream of visual processing sends signals to the parietal lobe comprising several higher-order cortical areas, such as the lateral intraparietal and ventral intraparietal areas that are known to constitute a dorsal attention network in concert with the association areas in the frontal lobe, such as the frontal eye field and dorsolateral prefrontal cortex (e.g., Corbetta & Shulman, 2002). Furthermore, extrastriate visual areas belonging to the dorsal pathway, such as area MT, may be capable of interactions between motion and position, because some of these areas possess the important combination of retinotopy, directional selectivity, attentional modulation, extrageniculate visual inputs, and feedback pathways to area V1. Hogendoorn, Verstraten, and Cavanagh (2015) reported that the very first electroencephalography (EEG) signals after visual stimulation already contained neural information about the subjective rather than physical position for the FGE, suggesting that dorsal extrastriate areas such as MT, rather than the areas in the frontal lobe, were responsible for these initial neural modulations in early visual areas. The present study also underscores the involvement of high-level processes, but cortical areas at anatomically high levels can evoke rapid visual responses that are sufficiently early in time to interact with the visual representations at anatomically early levels (e.g., Schmolesky et al., 1998). In contrast, the pattern of results in the present study cannot directly explain the contribution of monocular stages in the generation of the FGE as revealed by dichoptic experiments by van Heusden et al. (2019). Feedback signals from high-level attention-related processes to the monocular stages in the early visual cortex may well exist but cannot well explain the psychophysical signature of the monocular contribution, namely the attenuation of FGE in a dichoptic stimulus. However, our remark that high-level processes after the establishment of modal/amodal completion are involved in the FGE does not refute the hypothesis that there exists an additional process at a monocular stage that independently contributes to the FGE. For example, it cannot be refuted that interactions between motion and position also take place in subcortical loci, in particular the superior colliculus (Hogendoorn et al., 2015), where the ocular dominance distributions show a contralateral bias (Wallace, McHaffie, & Stein, 1997).

The present study reveals that the FGE can be formed on modally/amodally completed visual representations of the scene. Nevertheless, the question remains regarding what perceptual solution was actually taken in the case of amodal completion in our experiment, in which the blue ellipse appeared as occluding a part of the inducer that was thus invisible but understandable as continuously rotating behind. In the case of amodal completion (occluded inducer type), the perceived flash position, at least in the bottom-CCW condition, was well inside the ellipse, although the FGE was smaller than the one induced by the physical inducer. The same was true in the case of modal completion (filled-in inducer type). The reason why the flash should appear inside the ellipse is not obvious under the condition of amodal completion; why does the flash maintain its visibility there despite the amodal completion of the inducer per se, which ought to place the flash behind the occluder if the flash belongs to the inducer? Introspective reports indicated that the flash was rendered invisible in no trials. However, because it was also reported that the detailed stimulus layout was difficult to describe due to peripheral vision, possible phenomenological experiences could only be speculated. It is considered that the occluder, inducer, and flash can be phenomenologically ordered in depth in three possible ways: one, the flash does not belong to the inducer's surface but "floats" on top of it as another solitary object, so that the occluder covers only the inducer while the flash is "floating" in front of the occluder; two, the occluder simply covers both the flash and inducer, although the flash is a solitary object floating on top of the inducer; three, the occluder covers both the flash and inducer because they belong to the same rotating object behind the occluder. The solution to these ambiguities in the depth order is linked to the perceptual solution about the surface belongingness between the flash and inducer. In the first of the three scenarios, that is, if the flash and inducer are interpreted as independent objects sandwiching the occluder in between, the suddenly presented flash may be perceived as "floating" in front of the stable occluder. In contrast, the remaining two scenarios need more discussion. It is possible that the computations of depth order and localization proceed independently and in parallel; eventually, a perceptual interpretation that is consistent with both is created to reconcile the apparent discrepancy. One plausible phenomenology here may be that the occluded inducer "grabs" the flash behind the occluder, but the briefly presented red flash is "intense enough to transmit" through the blue ellipse because it can have a certain transmittance; therefore the red flash and blue ellipse are simultaneously visible, whereas the part of the inducer occluded by the ellipse remains invisible. Another possible phenomenological experience would be that some part of the flash "grabbed" by the inducer is horizontally "popping" or "peeking" out of the blue ellipse, contrary to the geometrical relationship on the display as the inducer only straddled the occluder vertically but never protruded it horizontally.

However, our participants found it difficult to tell whether such an event could be experienced against their knowledge that the flash was always superimposed on the inducer. This type of difficulty stems from our suboptimal spatial vision at the eccentricity at which the blind spot is located. In contrast, our discovery that the FGE can coexist with amodal completion opens the way to future experiments for investigating the interplay between the FGE prediction and the space occupied by an occluder in other parts of the visual field with better spatial resolution. For example, it is possible to investigate whether the flash subjectively overshoots the occluded space and is localized on the other side of it or whether the occluder's presence acts as some type of boundary constraining the spatial extent of position shifts. The present study does not answer this because we designed the experiment so that the FGE prediction should be placed inside the blind-spot or occluder region, not on the other side of it, based on previous studies reporting that the FGE amplitude can reach up to 10° of polar angle.

Factors affecting the position shift size

For both the filled-in and occluded inducer types, the FGE shift was >5° only in the bottom-CCW condition. In the group analysis, whereas the shift was >0° in the top-CW and top-CCW conditions, the shift did not significantly differ from 0° in the bottom-CW condition. These results contradicted the intuition that a typical FGE must be always observed when the inducer's boundary carrying the flash moved away from the obstacle (i.e., both the top-CCW and bottom-CW conditions).

The most likely reason why the bottom stimuli generally produced greater FGE amplitudes than the top stimuli would be the oblique effect because the bottom stimuli were presented down to the right in the periphery and presumably more susceptible to the illusory position shift whereas the top stimuli were closer to the horizontal meridian where finer spatial resolutions of sensory evidence tend to counteract the illusion. Alternatively, the FGE amplitude may become smaller there because the trajectory of the position shift has to cross the horizontal meridian. Another type of positional shift, the double-drift illusion, decreases when the meridian is present along its perceived path (Liu, Tse, and Cavanagh, 2018). This meridian hypothesis remains an interesting possibility but hardly explains why the effect was observed only in the cases of modal/amodal completion, whereas no statistical difference was found across conditions in the most classical stimulus configuration (physical inducer condition). One of the possible reasons for this discrepancy is that the spatiotemporal filling-in of the rotating inducer per se is affected by the horizontal meridian.

However, the oblique effect is not sufficient to fully explain why the *bottom-CW* condition yielded smaller FGE amplitudes than the bottom-CCW condition because the flash's physical position was identical between the two conditions. One possibility is a response bias toward the horizontal meridian, on which the blind spot, as well as our occluder, was located. However, this interpretation is ruled out because each participant was provided with a pre-training block to eliminate biases toward any particular polar angles. The reported polar angle against the actual polar angle of the flash in the practice trials indicates that there were no observable trends of angular responses biased toward any angles, let alone the horizontal meridian. Another possibility is that the blue ellipse covering the blind spot in the experiment using the filled-in inducer was not rendered completely invisible owing to miscalibration. If this had happened, the perceptual completion of the inducer might have been disrupted in an uncontrollable manner. However, this is unlikely because at the beginning of each block, it was confirmed that no part of the blue ellipse was visible and that the inducer appeared as fully completed across the blind spot. The third possible reason is that the positional precisions of the flash and/or probe were somehow higher around the blind spot than within it accompanied by filling-in. Recently, an EEG study measuring prediction error responses contingent on saccades toward and away from the blind spot (Ehinger, König, & Ossandón, 2015), as well as a psychophysical study on perceptual judgments for a stimulus eliciting filling-in of the blind spot and for an equivalent stimulus presented outside the blind spot (Ehinger et al., 2017), suggested that part of the visual system contains knowledge on the existence of a blind spot and makes use of it for planning and judgment. This hypothesis offers the idea that a map of visual defects made explicit in the retina and neurally represented in the early stages of visual processing, such as area V1, offers landmark information serving as a cue to relative position in the experiment with the filled-in inducer, just as the blue ellipse's visibility unquestionably served as a visual reference to the relative position in the experiment with the occluded inducer. It may be advantageous for the visual system to use innate anatomical structures as reference frames relative to which an object's position is elucidated. For example, consider the visual image of the nose; because it is always located at a fixed place, it may serve as a visible landmark (Wetherick, 1977). Likewise, other anatomically stable structures such as the blind spot might be able to provide spatial references for some internal computation even though the blind spot is invisible to the observer. To examine this possibility, we calculated the SD based on the distribution of the PSE data for each individual and submitted the SDs to the analysis of covariance with PSE as a covariate. However, we did not obtain a significant main effect of the presence/absence of perceptual filling-in, thus failing to identify systematic precision differences between conditions. Despite the lack of quantitative support from the current findings, the similarity between the results for the blind spot and occluder and the obvious spatial landmark provided by the occluder are suggestive of this claim, and future studies will be needed to optimize the experimental situation for specifically testing this intriguing possibility.

We tentatively interpret these asymmetrical data as a consequence of visual mechanisms. The crucial assumption is that the FGE occurs as a result of spatiotemporal integration of position within a limited time window spanning before and after the flash onset. A similar assumption is often made to account for position perception involving the flash (e.g., Krekelberg & Lappe 2000a; Krekelberg & Lappe 2000b; Roulston, Self, & Zeki, 2006; Sinico et al., 2009), and such a time window is supposedly open for several tens of milliseconds after the flash and presumably a much shorter time before the flash, the latter being causally implausible but allowed to exist under the assumption of stochastic latency fluctuations in visual responses. During the time window, the position of the moving stimulus is integrated to give the best estimate of the object position in relation to the flash (Brenner & Smeets, 2000; Whitney & Murakami, 1998; Whitney, Murakami, & Cavanagh, 2000), or the position of the flash itself in the FGE.

In the stimulus configuration of our experiment, however, it is likely that the boundary of the inducer in the vicinity of the blind spot has greater positional uncertainty in visual representation. From the report that the stripe density of a grating passing through the blind spot is underestimated (Revina & Maus, 2020), it is conceivable that a moving pattern subjectively filling in within the blind spot does not necessarily have the same accuracy and precision in space and time as the physically available pattern. When the inducer boundary in the bottom-CW condition is positionally integrated during the time window, the result is a mixture of the FGE away from the blind spot and a perceptual bias stemming from such a positional uncertainty of the perceptually completed pattern. Presumably, this bias may be directed toward the blind spot center rather than away from it, according to the abovementioned report on a subjective spatial distortion toward the blind spot center (Revina & Maus, 2020). While the FGE pulls the flash away from the blind spot, a high uncertainty behind the flash in a spatiotemporal window after the flash offset elongates the distribution of the flash's possible positions and biases its position toward the blind spot region (i.e., the direction opposite to the conventional FGE's).

When the inducer boundary in the bottom-CCW condition is integrated, the result is again a mixture of the FGE and the same bias, but because the FGE and the bias derived from this regional uncertainty are facing in the same direction, the bias does not hinder the FGE from occurring. The bias concept introduced here is not the response bias that was argued as an unlikely account, but the bias produced through the spatiotemporal integration of position. Nevertheless, this argument is still far from conclusive because it is an open question whether such an integrative computational process actually underlies the FGE.

In our experimental setup, the flash was 1.5 dva thick and positioned 5° away from the blind-spot region, and all participants confirmed that they never missed it. Nonetheless, future experiments using less salient stimuli should be conducted with additional procedures to quantify visibility if there is any doubt about it. Additionally, we tested the effect of the individual differences in the inducer width customized to each observer's blind spot. Still, we did not find any tendency of correlation between the inducer width and the FGE amplitude under any of the conditions (Pearson's $r \pm SE$: -0.045 ± 0.023).

Finally, the similar results under the async condition for a suboptimal FGE suggest that the sync and async conditions produced stronger and weaker versions of a qualitatively identical illusion of FGE. At the same time, we do not deny the view that the relationship between perceived position and modal/amodal completion in the present study is applicable to more general situations in which motion-induced position shifts occur. In our async condition, unidirectional motion inputs continue before and after the flash, causing the flash's apparent position to shift in the direction of motion. This stimulus configuration has a similarity to a typical configuration for the flash drag effect (FDE), although a flash does not belong to a moving stimulus as in our study but stands as an independent object in a classical setup of the FDE (Whitney & Cavanagh, 2000). The FDE occurs with occluded invisible motion (Watanabe, Sato, & Shimojo, 2003), supporting the involvement of relatively higher processes, in line with our results for the occluded inducer condition. The neural correlate of the FGE still remains unclear, although it has been reported that MT+ and V3A exhibit activation shifts corresponding to the flash position during FDE perception (Maus, Fischer, & Whitney, 2013). We expect that investigating the perceptual solutions we reach when various types of motion-induced positional shifts are pitted against perceptual completion provides crucial insights for elucidating visual processing involving position perception.

Conclusions

Even in monocular viewing, the visual scene should maintain a meaningful layout of objects for the observer to make sense of the environment. When a new object is registered within a scene, the visual system must make a quick estimation of its identity and spatiotemporal position. When a flash is suddenly lit at one of the boundaries of a moving luminance pattern, it takes a certain period of time for the flash appearance to be finalized in space and time of the visual world. If the pattern has moved by a certain distance, the visual system assumes that the flash is "grabbed" by this distance (Cavanagh & Anstis, 2013). If the pattern has moved onto the blind spot, the visual system assumes its permanence by exerting spatiotemporal filling-in from the sensory evidence of connection between visible parts of the pattern (Maus & Whitney; 2016). If the pattern has moved behind an occluder, the visual system assumes its permanence by solving perceived depth order from the occlusion cues (e.g., Kellman & Shipley, 1991). In this study, we reveal that none of these computational assumptions are reconsidered by the visual system even when the "grabbed" flash will fall inside the filled-in region of the blind spot or inside the occluded part of the moving inducer. This is true even if the perceptual solution of the flash position contradicts the visibility of the occluded part as in amodal completion. In principle, the FGE occurs just as predicted from a more typical, physically complete stimulus, although careful qualification in data evaluation, as well as future experimentation are necessary in a more quantitative aspect and generalizability across different polar angles, because the above conclusive remarks are statistically supported in a subset of data in this study.

Keywords: position, motion, flash grab effect, perceptual completion, blind spot

Acknowledgments

Supported by JSPS KAKENHI Grant Numbers JP18H01099, JP18H05523, JP23H01052, and JP23K25749.

Commercial relationships: none.
Corresponding author: Hoko Nakada.
Email: hokonakada@gmail.com.
Address: Department of Psychology, University of Tokyo, Tokyo 113-8654, Japan.

References

Adamian, N., & Cavanagh, P. (2024). Sustained attention and the flash grab effect. *Journal of Vision, 24*(2):6, 1–16, https://doi.org/10.1167/jov.24.2.6.

Awater, H., Kerlin, J. R., Evans, K. K., & Tong, F. (2005). Cortical representation of space around the blind spot. *Journal of Neurophysiology, 94*(5), 3314–3324, https://doi.org/10.1038/35075583.

Brainard, D. H. (1997). The Psychophysics Toolbox. *Spatial Vision, 10*, 433–436, https://doi.org/10.1163/156856897x00357.

Brenner, E., & Smeets, J. B. (2000). Motion extrapolation is not responsible for the flash-lag effect. *Vision Research, 40*(13), 1645–1648, https://doi.org/10.1016/S0042-6989(00)00067-5.

Cai, R., & Schlag, J.(2001). A new form of illusory conjunction between color and shape. *Journal of Vision, 1*(3):127, 127a, http://journalofvision.org/1/3/127/.

Cavanagh, P., & Anstis, S. (2013). The flash grab effect. *Vision Research, 91*, 8–20, https://doi.org/10.1016/j.visres.2013.07.007.

Coffey, K. M., Adamian, N., Blom, T., van Heusden, E., Cavanagh, P., & Hogendoorn, H. (2019). Expecting the unexpected: Temporal expectation increases the flash-grab effect. *Journal of Vision, 19*(13), 9, https://doi.org/10.1167/19.13.9.

Corbetta, M., & Shulman, G. L. (2002). Control of goal-directed and stimulus-driven attention in the brain. *Nature Reviews Neuroscience, 3*(3), 201–215, https://doi.org/10.1162/jocn_a_00281.

Cornelissen, F. W., Peters, E. M., & Palmer, J. (2002). The Eyelink Toolbox: eye tracking with MATLAB and the Psychophysics Toolbox. *Behavior Research Methods, Instruments, & Computers, 34*(4), 613–617, https://doi.org/10.3758/BF03195489.

de Hollander, G., van der Zwaag, W., Qian, C., Zhang, P., & Knapen, T. (2021). Ultra-high field fMRI reveals origins of feedforward and feedback activity within laminae of human ocular dominance columns. *NeuroImage, 228*, 117683, https://doi.org/10.1016/j.neuroimage.2020.117683.

Durant, S., & Johnston, A. (2004). Temporal dependence of local motion induced shifts in perceived position. *Vision Research, 44*(4), 357–366, https://doi.org/10.1016/j.visres.2003.09.022.

Eagleman, D. M., & Sejnowski, T. J. (2007). Motion signals bias localization judgments: A unified explanation for the flash-lag, flash-drag, flash-jump, and Frohlich illusions. *Journal of Vision, 7*(4):3, 1–12, https://doi.org/10.1167/7.4.3.

Ehinger, B. V., Häusser, K., Ossandon, J. P., & König, P. (2017). Humans treat unreliable filled-in percepts as more real than veridical ones. *Elife, 6*, e21761, https://doi.org/10.7554/eLife.21761.

Ehinger, B. V., König, P., & Ossandón, J. P. (2015). Predictions of visual content across eye movements and their modulation by inferred information. *Journal of Neuroscience, 35*(19), 7403–7413, https://doi.org/10.1523/JNEUROSCI.5114-14.2015.

Freyd, J. J., & Finke, R. A. (1984). Representational momentum. *Journal of Experimental Psychology: Learning, Memory, and Cognition, 10*(1), 126, https://doi.org/10.1037/0278-7393.10.1.126.

Fukiage, T., Whitney, D., & Murakami, I. (2011). A flash-drag effect in random motion reveals involvement of preattentive motion processing. *Journal of Vision, 11*(13), 12, https://doi.org/10.1167/11.13.12.

Hogendoorn, H., Verstraten, F. A., & Cavanagh, P. (2015). Strikingly rapid neural basis of motion-induced position shifts revealed by high temporal-resolution EEG pattern classification. *Vision Research, 113*, 1–10, https://doi.org/10.1016/j.visres.2015.05.005.

Kanizsa, G. (1955). Margini quasi-percettivi in campi con stimolazione omogenea. *Rivista di Psicologia, 49*, 7–13.

Kellman, P. J., & Shipley, T. F. (1991). A theory of visual interpolation in object perception. *Cognitive Psychology, 23*, 141–221, https://doi.org/10.1016/0010-0285(91)90009-D.

Kleiner, M., Brainard, D., & Pelli, D. (2007). What's new in Psychtoolbox-3? ECVP, conference abstract.

Koffka, K. (1935). *Principles of Gestalt Psychology*. New York: Harcourt, Brace.

Köhler, W. (1938). *The place of value in a world of facts*. New York: Liveright.

Komatsu, H., Kinoshita, M., & Murakami, I. (2000). Neural responses in the retinotopic representation of the blind spot in the macaque

V1 to stimuli for perceptual filling-in. *Journal of Neuroscience, 20*(24), 9310–9319, https://doi.org/10.1523/JNEUROSCI.20-24-09310.2000.

Komatsu, H., Kinoshita, M., & Murakami, I. (2002). Neural responses in the primary visual cortex of the monkey during perceptual filling-in at the blind spot. *Neuroscience research, 44*(3), 231–236, https://doi.org/10.1016/S0168-0102(02)00149-9.

Krekelberg, B., & Lappe, M. (2000a). A model of the perceived relative positions of moving objects based upon a slow averaging process. *Vision research, 40*(2), 201–215, https://doi.org/10.1016/S0042-6989(99)00168-6.

Krekelberg, B., & Lappe, M. (2000b). The position of moving objects. *Science, 289*(5482), 1107, https://doi.org/10.1126/science.289.5482.1107a.

Liu, S., Tse, P. U., & Cavanagh, P. (2018). Meridian interference reveals neural locus of motion-induced position shifts. *Journal of Neurophysiology, 119*(6), 2091–2099, https://doi.org/10.1152/jn.00876.2017.

Matsumoto, M., & Komatsu, H. (2005). Neural responses in the macaque V1 to bar stimuli with various lengths presented on the blind spot. *Journal of neurophysiology, 93*(5), 2374–2387, https://doi.org/10.1152/jn.00811.2004.

Maus, G. W., & Nijhawan, R. (2008). Motion extrapolation into the blind spot. *Psychological Science, 19*(11), 1087–1091, https://doi.org/10.1111/j.1467-9280.2008.02205.x.

Maus, G. W., & Whitney, D. (2016). Motion-dependent filling-in of spatiotemporal information at the blind spot. *PLoS One, 11*(4), e0153896, https://doi.org/10.1371/journal.pone.0153896.

Maus, G. W., Fischer, J., & Whitney, D. (2013). Motion-dependent representation of space in area MT+. *Neuron, 78*(3), 554–562, https://doi.org/10.1016/j.neuron.2013.03.010.

Merz, S., Soballa, P., Spence, C., & Frings, C. (2022). The speed prior account: A new theory to explain multiple phenomena regarding dynamic information. *Journal of Experimental Psychology: General, 151*(10), 2418–2436, https://doi.org/10.1037/xge0001212.

Metelli, F. (1985). Stimulation and perception of transparency. *Psychological Research, 47*(4), 185–202, https://doi.org/10.1007/BF00309446.

Müsseler, J., & Aschersleben, G. (1998). Localizing the first position of a moving stimulus: The Fröhlich effect and an attention-shifting explanation. *Perception & Psychophysics, 60*, 683–695, https://doi.org/10.3758/BF03206055.

Müsseler, J., & Kerzel, D. (2004). The trial context determines adjusted localization of stimuli: Reconciling the Fröhlich and onset repulsion effects. *Vision Research, 44*(19), 2201–2206, https://doi.org/10.1016/j.visres.2004.04.007.

Pelli, D. G. (1997). The VideoToolbox software for visual psychophysics: Transforming numbers into movies. *Spatial Vision, 10*, 437–442, https://doi.org/10.1163/156856897x00366.

Ramachandran, V. S. (1992). Blind spots. *Scientific American, 266*(5), 86–91.

Revina, Y., & Maus, G. W. (2020). Stronger perceptual filling-in of spatiotemporal information in the blind spot compared with artificial gaps. *Journal of Vision, 20*(4):20, 1–17, https://doi.org/10.1167/jov.20.4.20.

Roulston, B. W., Self, M. W., & Zeki, S. (2006). Perceptual compression of space through position integration. *Proceedings of the Royal Society B: Biological Sciences, 273*(1600), 2507–2512, https://doi.org/10.1098/rspb.2006.3616.

Scarfe, P., & Johnston, A. (2010). Motion drag induced by global motion Gabor arrays. *Journal of Vision, 10*(5), 14, https://doi.org/10.1167/10.5.14.

Schmolesky, M. T., Wang, Y., Hanes, D. P., Thompson, K. G., Leutgeb, S., Schall, J. D., . . . Leventhal, A. G. (1998). Signal timing across the macaque visual system. *Journal of Neurophysiology, 79*(6), 3272–3278, https://doi.org/10.1152/jn.1998.79.6.3272.

Sinico, M., Parovel, G., Casco, C., & Anstis, S. (2009). Perceived shrinkage of motion paths. *Journal of Experimental Psychology: Human Perception and Performance, 35*(4), 948–957, 10.1037/a0014257.

Sundberg, K. A., Fallah, M., & Reynolds, J. H. (2006). A motion-dependent distortion of retinotopy in area V4. *Neuron, 49*(3), 447–457, https://doi.org/10.1016/j.neuron.2005.12.023.

Takao, S., Sarodo, A., Anstis, S., Watanabe, K., & Cavanagh, P. (2022). A motion-induced position shift that depends on motion both before and after the test probe. *Journal of Vision, 22*(12):19, 1–15, https://doi.org/10.1167/jov.22.12.19.

Thornton, I. M. (2002). The onset repulsion effect. *Spatial vision, 15*(2), 219–244, https://doi.org/10.1163/15685680252875183.

Urale, P. W. B., Puckett, A. M., York, A., Arnold, D., & Schwarzkopf, D. S. (2022). Highly accurate retinotopic maps of the physiological blind spot in human visual cortex. *Human Brain Mapping, 43*(17), 5111–5125, https://doi.org/10.1002/hbm.25996.

van Heusden, E., Harris, A. M., Garrido, M. I., & Hogendoorn, H. (2019). Predictive coding of visual motion in both monocular and binocular human visual processing. *Journal of vision, 19*(1), 3, https://doi.org/10.1167/19.1.3.

Wallace, M. T., McHaffie, J. G., & Stein, B. E. (1997). Visual response properties and visuotopic representation in the newborn monkey superior colliculus. *Journal of Neurophysiology, 78*(5), 2732–2741, https://doi.org/10.1152/jn.1997.78.5.2732.

Ware, C. (1980). Coloured illusory triangles due to assimilation. *Perception, 9*, 103–107, https://doi.org/10.1068/p090103.

Watanabe, K. (2005). The motion-induced position shift depends on the visual awareness of motion. *Vision Research, 45*(19), 2580–2586, https://doi.org/10.1016/j.visres.2005.03.001.

Watanabe, K., Sato, T. R., & Shimojo, S. (2003). Perceived shifts of flashed stimuli by visible and invisible object motion. *Perception, 32*(5), 545–559, https://doi.org/10.1068/p5047.

Wertheimer, M. (1912). Experimentelle Studien über das Sehen von Bewegungen. *Zeitschrift für Psychologie und Physiologie der Sinnesorgane, 61*, 161–265.

Wetherick, N. E. (1977). The significance of the nose for certain phenomena of visual perception. *Nature, 266*(5601), 442–443.

Whitney, D., & Cavanagh, P. (2000). Motion distorts visual space: shifting the perceived position of remote stationary objects. *Nature neuroscience, 3*(9), 954–959, https://doi.org/10.1038/78878.

Whitney, D., & Murakami, I. (1998). Latency difference, not spatial extrapolation. *Nature neuroscience, 1*(8), 656–657, https://doi.org/10.1038/3659.

Whitney, D., Murakami, I., & Cavanagh, P. (2000). Illusory spatial offset of a flash relative to a moving stimulus is caused by differential latencies for moving and flashed stimuli. *Vision research, 40*(2), 137–149, https://doi.org/10.1016/S0042-6989(99)00166-2.

Supplementary material

Supplementary Movie S1. Stimuli that are identical for the filled-in inducer and occluded inducer types. Participants observed it with only the right eye open for the filled-in inducer and with both eyes open for the occluded inducer.

Supplementary Movie S2. Stimuli for the physical inducer type.

Supplementary Movie S3. Stimuli for uncompleted inducer type in the subsidiary experiment.